Available online at www.sciencedirect.com
ScienceDirect
Scripta Materialia 64 (2011) 430–433
Scripta MATERIALIA
www.elsevier.com/locate/scriptamat

Portevin–Le Chatelier (PLC) instabilities and slant fracture in C–Mn steel round tensile specimens

Huaidong Wang,[a,b,*] Clotilde Berdin,[a,c] Matthieu Mazière,[d] Samuel Forest,[d] Claude Prioul,[a] Aurore Parrot[b] and Patrick Le-Delliou[b]

[a] *Laboratoire de Mécanique des Sols, Structures et Matériaux, Grande Voie des Vignes, 92295 Châtenay-Malabry, France*
[b] *Electricité de France, R&D Division, Département MMC, Les Renardières, 77818 Moret-sur-Loing Cedex, France*
[c] *Université Paris-Sud 11, ICMMO, LEMHE 91, France*
[d] *Centre des Matériaux, Mines ParisTech CNRS UMR 7633 BP 87, F-91003 Evry Cedex, France*

Received 1 October 2010; revised 1 November 2010; accepted 2 November 2010
Available online 8 November 2010

Round tensile specimens of a C–Mn steel were tested at different strain rates and temperatures. Some of the samples tested in the Portevin–Le Chatelier (PLC) domain exhibit slant fracture surfaces. Spherical dimples were evidenced all over the slant fracture surfaces. Numerical simulations showed that stress triaxiality increases around PLC bands and that slant fracture occurs within a PLC band. In a round specimen, this band is plane and inclined, whereas some numerical results predict conical bands.

Keywords: Portevin–Le Chatelier instabilities; Fracture surfaces; Numerical modeling; Band orientation

Ferritic steels such as C–Mn steels are sensitive to dynamic strain ageing at around 200 °C under quasi-static loading [1–4]. Dynamic strain ageing affects the strain-rate sensitivity (SRS) of the material and induces a jerky flow [5], the so-called "Portevin–Le Chatelier" (PLC) effect. Dynamic strain ageing also results in a decrease in fracture toughness [1–4]. Hence, it is important to predict this phenomenon for safety analyses when the phenomenon occurs at the service temperature of a component made from C–Mn steel. As a first step, the PLC effect with the associated strain localizations has to be predicted for tensile tests.

Recently, some authors predicted by numerical simulations that the PLC strain localization bands in round smooth specimens are rather conical [6,7]. This is questionable since slantwise fracture is observed in round smooth specimens [4]. Furthermore, some authors [8] claim that there is no correlation between fracture and PLC bands for plate specimens. However, it is difficult to reach definitive conclusions because, in plates, strain localization (even without dynamic strain ageing) occurs at an angle of about 54° to the tensile axis, as was demonstrated by McClintock and Argon [9]. Theoretical study shows that strain localization in round specimens can be axisymmetric (conical) or slanted [10]. In addition, using a finite-element method, Mazière et al. [11] showed that PLC bands could be either inclined or conical in round smooth specimens depending on the macroscopic strain rate.

There are many observations of strain localization bands due to the PLC phenomenon in flat specimens of aluminium alloys [8,12–14] evidenced by digital image correlation (DIC) and infrared thermography. In fact, for aluminium alloys, the PLC effect occurs at room temperature and it is easy to make observations on flat specimens. For steels, the PLC effect occurs at intermediate temperatures (around 200 °C). At these temperatures, it is difficult to observe PLC bands on steels with available experimental methods, especially for round specimens due to their curved surfaces. Hence, there have in fact been no observations of PLC bands in steels, either on flat specimens or on round ones.

In this paper, the morphology of PLC strain localization bands in round specimens and its relation to slant fracture are carefully studied by experiments that involve characterization of the fracture surface and numerical modeling with a suitable strain ageing model:

* Corresponding author at: Laboratoire de Mécanique des Sols, Structures et Matériaux, Grande Voie des Vignes, 92295 Châtenay-Malabry, France. Tel.: +33 1 41 13 15 16; fax: +33 1 41 13 14 30; e-mail: huaidong.wang@ecp.fr

1359-6462/$ - see front matter © 2010 Acta Materialia Inc. Published by Elsevier Ltd. All rights reserved.
doi:10.1016/j.scriptamat.2010.11.005

the Kubin–Estrin–McCormick (KEMC) model, which is presented in detail in the work of Belotteau et al. [4]. The model was used to simulate the mechanical behavior of a C–Mn steel in the presence of strain ageing [4]. In this work, we propose to model round specimens with full three-dimensional (3-D) computation in order to simulate inclined bands if they exist and to correlate inclined PLC bands and slant fracture surfaces.

The material studied is a C–Mn steel which was presented in Ref. [4]. In the previous study, 14 tensile tests were carried out at two strain rates (10^{-2} and $10^{-4}\,s^{-1}$) and seven temperatures, from 20 to 350 °C, in order to characterize the mechanical behavior of the material and to identify the KEMC model over a large temperature range. The specimens used were round smooth specimens with a gauge length of 36 mm and a diameter of 6 mm. In this study, an additional 10 tensile specimens were tested at 10^{-3} and $10^{-5}\,s^{-1}$ at the same temperatures to enlarge the experimental database, in order to improve the identification of some key parameters of the KEMC model, which are related to strain ageing.

The thermally activated elastoviscoplastic model derives from models proposed by Estrin and Kubin [5] and McCormick [15]. It was first proposed by Zhang et al. [6] and adapted by Graff et al. [16]. The model was identified by Belotteau et al. [4]. Some of the parameters, especially the parameters of the strain-ageing hardening, were modified in this study with supplementary experimental data in order to underline the material parameter dependence of simulation results concerning PLC instabilities in 3-D round specimens.

In the KEMC model, an internal variable, the ageing time t_a, was introduced to model the overhardening due to the strain ageing. Higher values of t_a induce stronger overhardening up to a limit value. Its evolution law depends on equivalent plastic strain rate ($\dot{p}$) through the parameter ω, which is the strain increment produced when all arrested dislocations overcome localized obstacles and advance to the next pinned configuration:

$$\dot{t}_a = 1 - \frac{\dot{p}}{\omega} t_a \quad t_a(t=0) = t_{a0}. \tag{1}$$

According to Estrin and Kubin [5], the parameter ω evolves with strain: it increases rapidly and attains a peak value at a small strain, decreases slowly and tends to an asymptotic value. Here, for the sake of simplicity, the parameter ω was taken as a constant as done in Refs. [7,11,16]. In these numerical simulations of PLC effect, ω was equal to 10^{-4}.

Figure 1 displays the influence of ω on the ageing time evolution with respect to the equivalent plastic strain at 200 °C and $10^{-4}\,s^{-1}$ on a representative elementary volume. Ageing time t_a was normalized by the waiting time $t_w = \omega/\dot{p}$ (time spent by a mobile dislocation pinnned by obstacles, before overcoming them). The ageing time depends on the equivalent accumulated plastic strain: first, it increases, reaches the limit value and then decreases to zero, at which point a strain localization arises. In the first stage, the material evolves from a fully unpinned state to a fully pinned state. In the second stage, when a PLC band (strain rate band) passes by, the material evolves from a fully pinned state to a fully unpinned state. It is important to note that ω has a significant influence on the transition process between these two extreme states: decrease of ω accelerates the transition process. Hence, decreasing this value probably promotes strain localization.

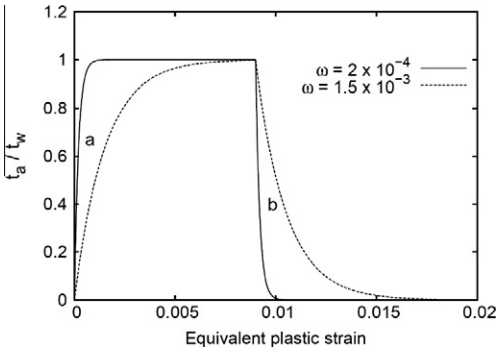

Figure 1. Influence of ω on the ageing time evolution at 200 °C and $10^{-4}\,s^{-1}$ for $\omega = 1.5 \times 10^{-3}$ and $\omega = 2 \times 10^{-4}$ on a representative elementary volume: (a) evolution from a fully unpinned state to a fully pinned state; (b) evolution from a fully pinned state to a fully unpinned state.

Two numerical simulations of tensile test on a round specimen were carried out using the KEMC model at $10^{-4}\,s^{-1}$ and 200 °C with the two different values of ω: 2×10^{-4} and 1.5×10^{-3}. The elements used are eight-node quadratic elements with reduced integration. Figure 2 shows the contour values of plastic strain rate. Figure 2a is the simulation result with $\omega = 1.5 \times 10^{-3}$; in Figure 2b $\omega = 2 \times 10^{-4}$. Two shapes of PLC bands were obtained with the two different values of ω. For the higher value of ω, the PLC band is diffuse and appears horizontal (it is conical within the volume (Fig. 2a (right)), whereas for the lower value of ω, the PLC band is much more localized and it is inclined (Fig. 2b). The types of bands can be determined by their spatiotemporal occurrence. A numerical indicator, the BLI (Band Location Indicator), was developed for that purpose in Ref. [11]. From Ref. [11], conical bands and inclined bands could be attributed to A–B type according to the BLI analysis. Figure 2c represents the necking state corresponding to case (b). It can be seen that necking initiated inside a PLC band.

Figure 3a represents the fracture surface profiles (axial section) and the PLC serration types of all the specimens tested. The triangles represent slant fracture surfaces, whereas the other symbols represent cup and cone fracture surfaces. The three colours correspond to the three types of PLC serrations and the blank symbols mean that no PLC serrations were observed on the tensile curve. From the experimental results, it was found that, for the C–Mn steel, the PLC effect appears between 150 and 300 °C for the four strain rates. The distribution of the three types of PLC bands (identified from PLC serrations on the tensile curves) is classical: at a fixed temperature, the sequence is C–B–A for increasing strain rate; at a fixed strain rate, the sequence is A–B–C for increasing temperature [17].

Another simulation was carried out at $10^{-3}\,s^{-1}$, a higher strain rate, at 200 °C with $\omega = 2 \times 10^{-4}$ using the KEMC model. Two PLC bands were observed at the same time and these two bands are of type A–B

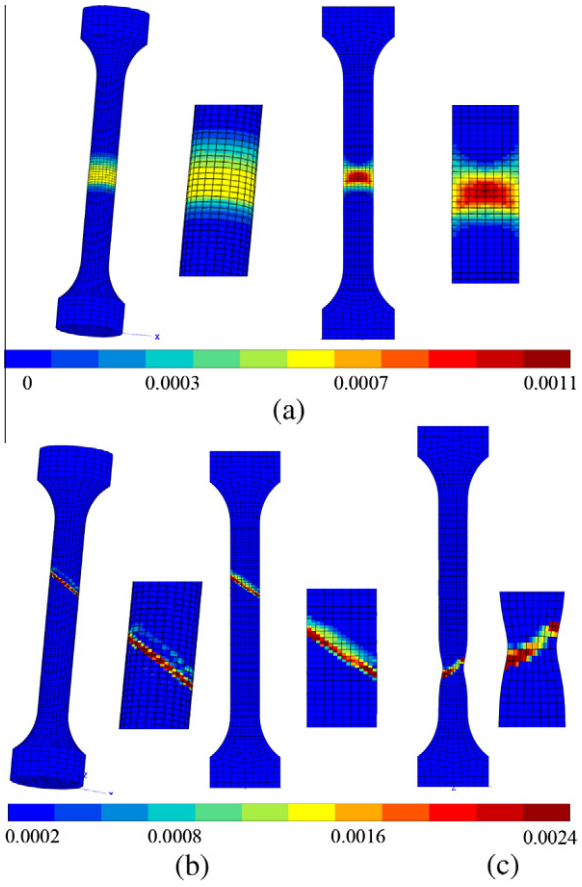

Figure 2. Field of equivalent plastic strain rate (s^{-1}) during strain localization for two different values of ω at 200 °C and 10^{-4} s^{-1} (the PLC bands are enlarged to show the details): (a) $\omega = 1.5 \times 10^{-3}$ (exterior surface and longitudinal section); (b) $\omega = 2 \times 10^{-4}$ (exterior surface and longitudinal section); (c) necking within a PLC band (longitudinal section).

according to the BLI analysis. In addition, the PLC bands are initially inclined and then assume a conical shape. Therefore, from the point of view of morphology, there are two forms of PLC band depending on strain rate: inclined or conical. Mazière et al. have already reported this phenomenon [11].

Some specimens, such as those tested at 10^{-4} or 10^{-5} s^{-1} at 200 °C, exhibit a slantwise fracture surface, whereas others exhibit the typical features of a cup–cone fracture surface [18]. From Figure 3a, it is found that slant fracture surfaces correspond to type B and C PLC serrations. In addition, type A serrations lead to cup–cone fracture surfaces. At 200 °C, comparing the simulations and experimental results, we found that there is a close relationship between band morphologies and fracture surfaces: inclined bands (10^{-4} s^{-1}) for slant fracture surfaces and conical bands (10^{-3} s^{-1}) for cup–cone fracture surfaces. There is also a relationship between band types and fracture surfaces: type B and C bands for slant fracture surfaces and type A bands for cup–cone fracture surfaces.

Fractographic analysis was performed to determine the underlying mechanisms of the slant fracture. Figure 3b (left) shows the global observation of the fracture surface of the specimen tested at 10^{-5} s^{-1} and 200 °C. As previously mentioned, the fracture surface is slanted.

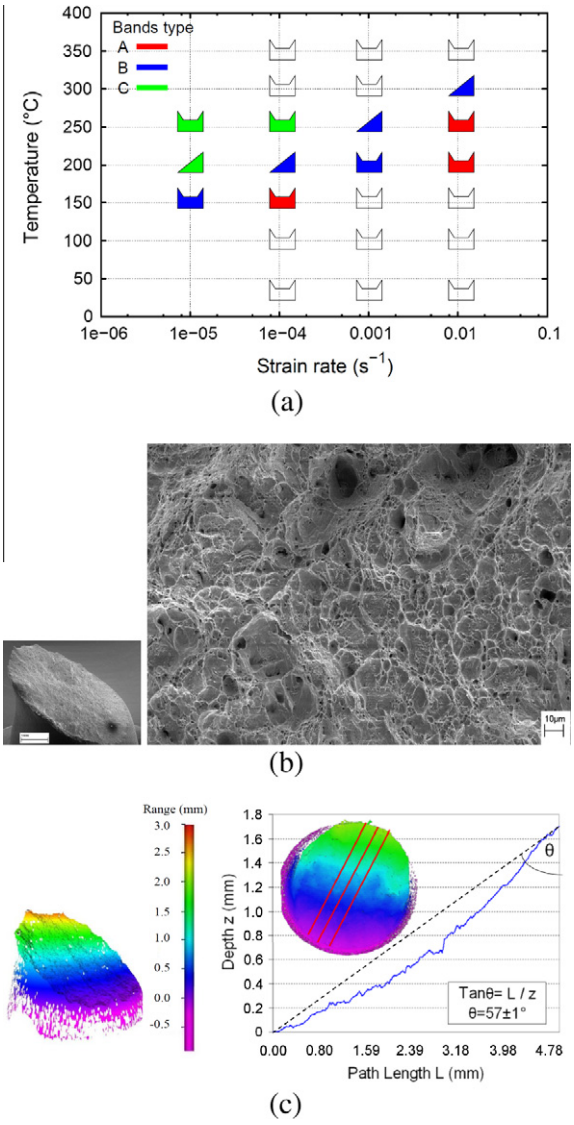

Figure 3. (a) Fracture surfaces distribution of all tested specimens; (b) global and local view (SEM) of the fracture surface of the specimen tested at 10^{-5} s^{-1} and 200 °C; (c) 3-D analysis of the fracture surface of the specimen tested at 10^{-5} s^{-1} and 200 °C with a microtoposcope.

Images of the fracture surface were taken at different focus points with an Alicona Microtoposcope. Using software which automatically identifies the focused points and constructs 3-D topological images, the angle between the specimen axis and the slant surface was found to be close to 57° (see Fig. 3c). The entire surface was carefully analysed by scanning electron microscopy (SEM). Under combined hydrostatic stress and shear stress conditions, as encountered in the edge part of a cup–cone fracture surface, voids take an elliptic shape because they are simultaneously enlarged and sheared in the shear stress direction [18]. Figure 3b (right) shows one of the local zones of the slanted surface. The dimples are rather spherical even though the surface is inclined as in shear fracture: no shear evidence was found, which means that the fracture is caused by the growth and coalescence of voids under a triaxial stress state.

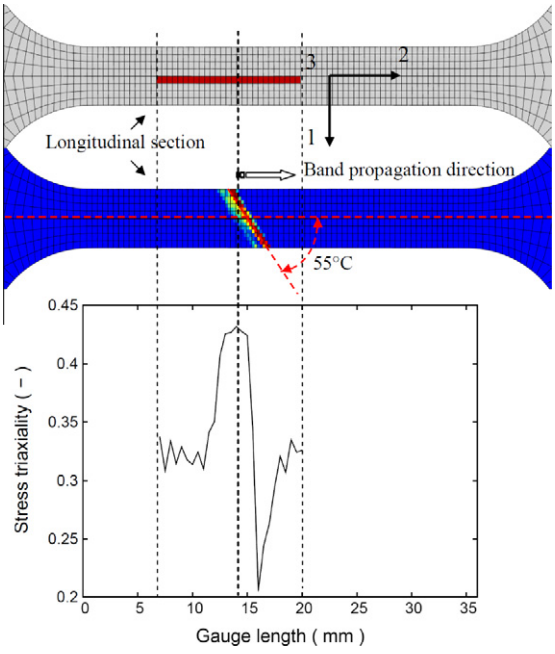

Figure 4. Evolution of stress triaxiality ratio along the tensile axis at 200 °C and $10^{-4}\,s^{-1}$.

Figure 4 displays the evolution of the stress triaxiality of the Gauss point close to the tensile axis of a series of elements indicated in the red zone of the mesh for the simulation carried out at $10^{-4}\,s^{-1}$ and 200 °C with $\omega = 2 \times 10^{-4}$. The orientation angle of the PLC band on the contour value of the equivalent plastic strain rate with respect to the tensile axis is about 55°, which is close to that of the slantwise fracture surface (Fig. 3c). From Figure 4, it can be seen that the stress triaxiality ratio reaches its maximal value slightly behind the PLC band. Theoretical analysis of strain localization in a plate specimen shows that the slant band is submitted to uniaxial tension [9]. This is not the case for slant bands in round specimens since stress triaxiality within the band is close to 0.45, which is higher than 0.33 for the case of uniaxial tension. This probably favours damage by growth of voids in a PLC band and causes necking within a PLC band (see Fig. 2c).

All the results presented above lead to the conclusion that the ductile fracture of a round tensile specimen which exhibits a slantwise fracture surface is due to the growth and coalescence of voids within an inclined PLC band. For the modeling of such bands with the KEMC model, it is imperative to correctly identify the parameter ω with full 3-D computations: a value that is too high leads to conical bands in round specimens that are not in agreement with our experimental observations.

[1] D. Wagner, J.C. Moreno, C. Prioul, J. Nucl. Mater. 252 (1998) 257–265.
[2] D. Wagner, J.C. Moreno, C. Prioul, J.M. Frund, B. Houssin, J. Nucl. Mater. 300 (2002) 178–191.
[3] K.C. Kim, J.T. Kim, J.I. Suk, U.H. Sung, H.K. Kwon, Nucl. Eng. Des. 228 (2004) 151–159.
[4] J. Belotteau, C. Berdin, S. Forest, A. Parrot, C. Prioul, Mater. Sci. Eng., A 526 (2009) 156–165.
[5] Y. Estrin, L.P. Kubin, in: Continuum Models for Materials with Microstructure, John Wiley and Sons, New York, 1995, p. 422.
[6] S. Zhang, P.G. McCormick, Y. Estrin, Acta Mater. 49 (2001) 1087–1094.
[7] A. Benallal, T. Berstad, T. Borvik, O.S. Hopperstad, I. Koutiri, R. Nogueira De Codes, Int. J. Plasticity 24 (2008) 1916–1945.
[8] H. Halim, D.S. Wilkinson, M. Niewczas, Acta Mater. 55 (2007) 4151–4160.
[9] F.A. McClintock, A.S. Argon, Mechanical Behavior of Materials, Addison-Wesley, Reading, MA, 1966, pp. 321–322.
[10] J.W. Rudnicki, J.R. Rice, J. Mech. Phys. Solids 23 (1975) 371–394.
[11] M. Mazière, J. Besson, S. Forest, B. Tanguy, H. Chalons, F. Vogel, Comput. Methods Appl. Mech. Eng. 199 (2010) 734–754.
[12] H. Louche, P. Vacher, R. Arrieux, Mater. Sci. Eng., A 404 (2005) 188–196.
[13] N. Ranc, D. Wagner, Mater. Sci. Eng., A 474 (2008) 188–196.
[14] H. Ait-Amokhtar, C. Fressengeas, S. Boudrahem, Mater. Sci. Eng., A 488 (2008) 540–546.
[15] P.G. McCormick, Acta Metal. 36 (1988) 3061–3067.
[16] S. Graff, S. Forest, J.-L. Strudel, C. Prioul, P. Pilvin, J.-L. Béchade, Mater. Sci. Eng., A 387–389 (2004) 181–185.
[17] J.L. Strudel, in: Dislocations et déformation plastique, Ecole d'ete d'Yravals, 1979, Les éditions de physique, 1979, p. 199.
[18] P.F. Thomason, Ductile Fracture of Metals, Pergamon Press, Oxford, 1990.